Structural Eng. / Earthquake Eng. Vol. 5. No. 1, 89s-97s. April 1988
Japan Society of Civil Engineers (Proc. of JSCE No. 392/I-9)

LOCAL STRESSES AT CROSS BEAM CONNECTIONS OF PLATE GIRDER BRIDGES

By Ichiro OKURA, Masao YUBISUI**, Hiroshi HIRANO*** and Yuhshi FUKUMOTO*****

It has been reported that fatigue cracks were often initiated at the connections of cross beams to main girders in plate girder bridges. In this paper, the relation between the local stresses which induced the fatigue cracks and the three-dimensional behavior of plate girder bridges is formulated by the results of the stress measurement of an actual plate girder bridge and its three-dimensional finite element analysis. The obtained equation reveals the influential factors for the occurrence of the local stresses.

Keywords : fatigue, plate girder bridge, F. E. M. analysis, connection

1. INTRODUCTION

Recently, it has been reported in Japan and abroad that many welded steel bridges have fatigue cracks at the connections of secondary members to main members[1)~3)]. In the case of plate girder bridges, as shown in Fig. 1, four types of fatigue cracks occur at the connections of cross beams to main girders[4)].

Type 1 fatigue crack : This is initiated either on the bead or at the toe at the end of the fillet weld between the connection plate and the top flange of the main girder.

Type 2 fatigue crack : This is initiated at the upper scallop of the connection plate, and grows diagonally through the connection plate itself.

Type 3 fatigue crack : This is initiated at the toe at the end of the fillet weld connecting the connection plate to the main girder web, and grows downward along the toe on the connection plate side.

Type 4 fatigue crack : This is initiated and grows along the toe on the web side of the fillet weld between the top flange and the web of the main girder.

The order of initiation of the fatigue cracks among four types is not clear. The investigation of the cause of

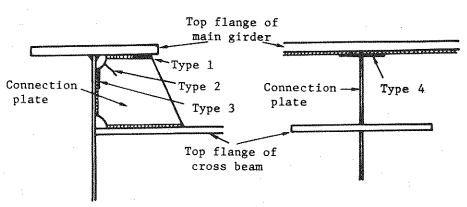

Fig. 1 Fatigue cracks at cross beam connection.

* Member of JSCE, Dr. Eng., Research Associate, Department of Civil Engineering, Osaka University (Yamadaoka 2-1, Suita, Osaka 565)
** Member of JSCE, Graduate Student, Department of Civil Engineering, Osaka University
*** Member of JSCE, M. Eng., Civil Engineering Bureau, Osaka Prefectural Government (Otemae, Higashiku, Osaka 540)
**** Member of JSCE, Ph. D., Dr. Eng., Professor, Department of Civil Engineering, Osaka University

initiation of the fatigue cracks and the development of repair methods for them are now under way at various research institutes[5)~7)]. However, comprehensive results are not yet given.

The difference in vertical displacement between main girders and the deformation of a concrete slab are pointed out as the main causes of the fatigue cracks[8),9)]. However, it is not made clear how these factors are related to the local stresses which induce the fatigue cracks.

We carried out the stress measurement of an actual plate girder bridge, and examined in depth the stress state at the connections of the cross beam to the main girders to show the local stresses governing the initiation of the fatigue cracks[10)]. The object of this paper is to obtain the relation between the local stresses and the three-dimensional behavior of the plate girder bridge. First, a linear equation is assumed among the local stresses, the rotations and horizontal displacements of the slab and cross beam. Secondly, using the results of the stress measurement of the plate girder bridge and of its three-dimensional finite element analysis, the undetermined coefficients in the equation are determined by the least squares method. Lastly, the influential factors for the occurrence of the local stresses are revealed by the equation.

2. EQUATION TO ESTIMATE LOCAL STRESSES AT CROSS BEAM CONNECTION

(1) Model to estimate local stresses

It was shown from the stress measurement of an actual plate girder bridge that the membrane stress σ_{my} and the plate-bending stress σ_{by}, as illustrated in Fig. 2, were the governing stresses for the initiation of Types 1 and 4 fatigue cracks, respectively[10)]. They would be caused by the respective rotations about the bridge-axis of the concrete slab and cross beam at the connection of the cross beam to the main girder and by their respective horizontal displacements in the direction perpendicular to the bridge-axis. Referring to Fig. 3, let us assume that the membrane stress σ_{my} or the plate-bending stress σ_{by} has a linear relation with these factors, as expressed by the following equation.

$$\begin{bmatrix}\sigma_{my}\\ \sigma_{by}\end{bmatrix}=\begin{bmatrix}k_{m1} & k_{m2} & k_{m3}\\ k_{b1} & k_{b2} & k_{b3}\end{bmatrix}\begin{bmatrix}\theta_s\\ \theta_g\\ \Delta u_{sg}\end{bmatrix} \quad \cdots\cdots (1)$$

where $\Delta u_{sg}=u_s-u_g$, θ_s and u_s are, respectively, the rotation and the horizontal displacement defined on the middle surface of the slab, θ_g and u_g are, respectively, the rotation and the horizontal displacement defined at the neutral axis of the cross beam, and $k_{m1}\sim k_{m3}$, $k_{b1}\sim k_{b3}$ are coefficients.

As given by the following equation, the rotation θ_s of the slab can be divided into the rotation θ_{s0} due to the plate-bending deformation of the slab under the condition that the main girders do not deflect vertically and the rotation θ_{s1} produced by the vertical displacements of the main girders.

$$\theta_s=\theta_{s0}+\theta_{s1} \quad \cdots\cdots (2)$$

Substituting Eq. (2) into Eq. (1), the following equation is obtained.

$$\begin{bmatrix}\sigma_{my}\\ \sigma_{by}\end{bmatrix}=\begin{bmatrix}k_{m1} & k_{m1} & k_{m2} & k_{m3}\\ k_{b1} & k_{b1} & k_{b2} & k_{b3}\end{bmatrix}\begin{bmatrix}\theta_{s0}\\ \theta_{s1}\\ \theta_g\\ \Delta u_{sg}\end{bmatrix} \quad \cdots\cdots (3)$$

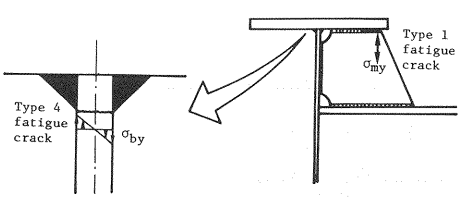

Fig. 2 Fatigue crack types and local stresses.

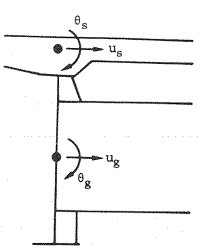

Fig. 3 Notation.

In Eq. (3), the first term on the right side gives the local stress component produced by the plate-bending deformation of the slab, and the second to fourth terms give the local stress components due to the three-dimensional behavior of the bridge.

(2) Formulation of θ_{s0}

As mentioned in the preceding section, θ_{s0} is the rotation of a slab due to its plate-bending deformation under the condition that main girders do not deflect vertically. As shown in Fig. 4, when a concentrated load P acts at the arbitrary point (x, y) on an infinitely long plate which is simply supported on two opposite edges, the rotations about the y-axis at the points 1 and 2 are given by the following equations[11].

$$\theta_{y1}(x, y)=\frac{Pa}{2\pi^2 D}\sum_{m=1}^{\infty}\frac{1}{m^2}\sin\frac{m\pi x}{a}\left(1+\frac{m\pi|y|}{a}\right)e^{-\frac{m\pi|y|}{a}} \quad (4)$$

$$\theta_{y2}(x, y)=\frac{Pa}{2\pi^2 D}\sum_{m=1}^{\infty}\frac{(-1)^m}{m^2}\sin\frac{m\pi x}{a}\left(1+\frac{m\pi|y|}{a}\right)e^{-\frac{m\pi|y|}{a}} \quad (5)$$

where θ_{y1} and θ_{y2} are the rotations about the y-axis at the points 1 and 2, respectively, D is the flexural rigidity of the plate, a is the interval between the supporting edges, and m is integer.

Taking a cross beam on the x-axis in Fig. 4, the equation to estimate θ_{s0} for plate girder bridges supported by two main girders with a spacing of a is given by Eqs. (4) and (5). The variation of θ_{y1} as the load is away along $x=a/2$ from the cross beam is shown in Fig. 5. It can be seen from the figure that θ_{y1} is almost zero when the load is away from the cross beam by more than $2a$. Accordingly, when the load is away from the cross beam by more than two times the main girder spacing, the influence of the load on θ_{s0} can be neglected.

Next, let us consider the equation to estimate θ_{s0} for plate girder bridges with more than two main girders. A continuous plate which is simply supported on five lines is shown in Fig. 6. Letting the rotations at the points 1, 2 and 3 on the supporting lines be denoted by θ_{s01}, θ_{s02} and θ_{s03}, respectively, they are given by the following equations by examining the ratios of the rotations at these points obtained from the finite element analysis to the ones given by Eqs. (4) and (5).

a) When the concentrated load P is between the supporting lines of G_1 and G_2,

$$\theta_{s01}=\phi_{12}\theta_{y1}(x_{12}, y) \quad (6)$$

$$\theta_{s02}=\phi_{21}\theta_{y2}(x_{12}, y) \quad (7)$$

where $\phi_{12}=-0.475\, x_{12}/a+1.034$, $\phi_{21}=0.030\, x_{12}/a+0.470$, and x_{12} is the distance from the supporting line G_1.

b) When the concentrated load P is between the supporting lines of G_2 and G_3,

$$\theta_{s02}=\phi_{23}\theta_{y1}(x_{23}, y) \quad (8)$$

$$\theta_{s03}=\phi_{32}\theta_{y2}(x_{23}, y) \quad (9)$$

where $\phi_{23}=-0.237\, x_{23}/a+0.533$, $\phi_{32}=0.228\, x_{23}/a+0.289$, and x_{23} is the distance from the supporting line G_2. A comparison of the results from Eq. (7) with the ones from the finite element analysis is shown in Fig. 7. It can be seen that Eq. (7) approximates very well the values from the finite element analysis.

The variation of θ_{s01} as the concentrated load moves on the x-axis toward the supporting line G_3 from G_1

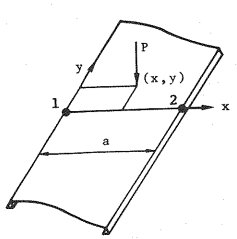

Fig. 4 Simply supported infinitely long plate.

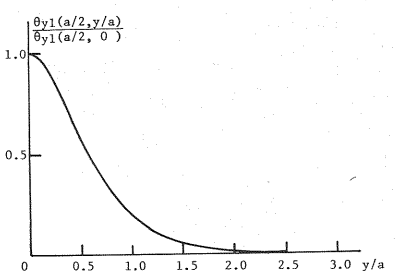

Fig. 5 Variation of θ_{y1}.

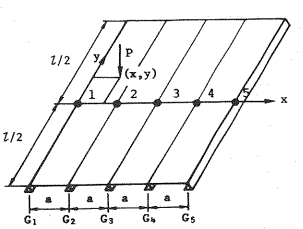

Fig. 6 Four span continuous plate.

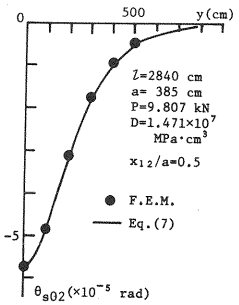

Fig. 7 Comparison between the results of Eq. (7) and of the finite element analysis.

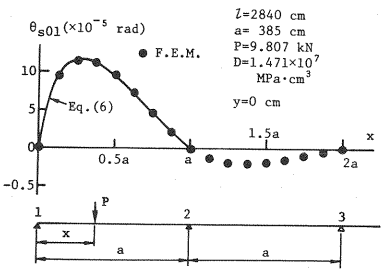

Fig. 8 Variation of θ_{s01}.

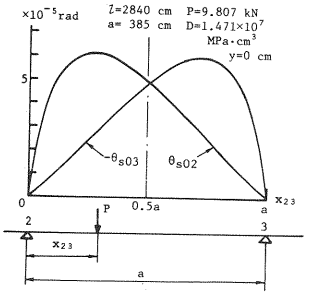

Fig. 9 Comparison between θ_{s02} and $-\theta_{s03}$.

is shown in Fig. 8. Equation (6) approximates very well the values from the finite element analysis between the supporting lines of G_1 and G_2. The values of θ_{s01} when the load is between the supporting lines of G_2 and G_3 are much smaller than those when it is between the supporting lines of G_1 and G_2.

As can be seen from Fig. 9, when the concentrated load is between the supporting lines of G_2 and G_3, the variation of θ_{s02} is almost symmetrical with that of $-\theta_{s03}$ about $x_{23}=0.5\,a$. That is to say, the rotations θ_{s02} and θ_{s03} are mainly influenced by the adjoining spans on both sides of the G_2-G_3 span and not influenced by the G_4-G_5 span.

From the above-mentioned consideration, as the equation to estimate θ_{s0} for plate girder bridges with more than two main girders, Eqs. (6) and (7) will be used when wheel loads are on the slab on exterior spans, and Eqs. (8) and (9) used when they are on the slab on interior spans.

(3) Relation between θ_g and vertical displacements of main girders

The rotation θ_g of the cross beam at the connection of the cross beam to the main girder can be expressed by the vertical displacements of the main girders from the theory of structures. In the case of five main girders, it is given by

$$\begin{bmatrix}\theta_{g1}\\ \theta_{g2}\\ \theta_{g3}\\ \theta_{g4}\\ \theta_{g5}\end{bmatrix}=\frac{1}{56\,a}\begin{bmatrix}-71 & 90 & -24 & 6 & -1\\ -26 & -12 & 48 & -12 & 2\\ 7 & -42 & 0 & 42 & -7\\ -2 & 12 & -48 & 12 & 26\\ 1 & -6 & 24 & -90 & 71\end{bmatrix}\begin{bmatrix}v_1\\ v_2\\ v_3\\ v_4\\ v_5\end{bmatrix} \quad \cdots\cdots (10)$$

where $\theta_{g1}\sim\theta_{g5}$ are the rotations of the cross beam at the connections of the cross beam to the main girders, and $v_1\sim v_5$ are the displacements of the main girders with the downward direction positive.

3. DETERMINATION OF COEFFICIENTS $k_{m1}\sim k_{m3}$, $k_{b1}\sim k_{b3}$ IN EQ. (3)

(1) General view of plate girder bridge[10]

The plate girder bridge on which the stress measurement was carried out is shown in Fig. 10. It is a simply-supported composite plate girder bridge with a span length of 28.4 m and total width of 17.6 m, which was designed by the Japanese Specification for Highway Bridges[12]. The bridge has five main girders, a cross beam in the middle of the span and six sway bracings. The concrete slab is 180 mm thick. The bridge was opened to traffic in 1970. Repair and reinforcement works for the slab were done in 1979. A steel plate 4.5 mm thick was attached to the bottom surface of the slab, and as shown by dotted lines in Fig. 10, one stringer between G_4 and G_5 girders, two stringers between G_3 and G_4 girders, and one stringer in part between G_1 and G_2 girders were installed.

The loading truck and its loading positions are shown in Figs. 11 and 12, respectively. Four cases of A,

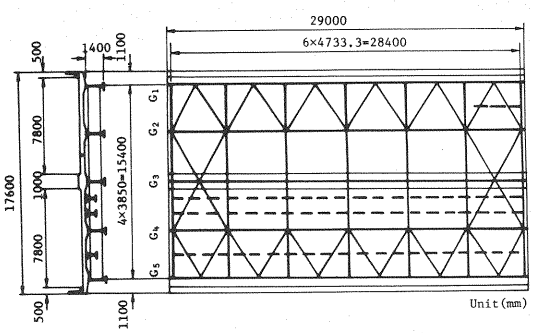

Fig. 10 General view of plate girder bridge.

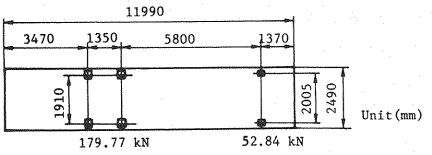

Fig. 11 Loading truck,

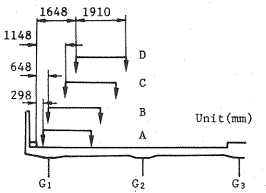

Fig. 12 Loading positions of truck.

B, *C* and *D* were taken up according to the intervals between the coping and the center of rear double-tires on the left side. The static stress measurement was carried out at 11 locations in the bridge-axis direction for each loading case. 24 one-directional, 214 two-directional and 126 three-directional strain gauges were attached on the cross beam connections at G_1 and G_2 girders.

(2) Three-dimensional finite element analysis of plate girder bridge

The three-dimensional behavior of the plate girder bridge on which the stress measurement was carried out is analysed by the finite element method. The mesh division of each member is as follows.

a) The slab is divided into quadrilateral plate elements[13] with in-plane and out-of-plane displacements.

b) As for the main girders, end sway bracings and stringers, the top flange is neglected, and the web is assumed to be jointed rigidly with the slab. The web is divided into quadrilateral plate elements with in-plane and out-of-plane displacements, while the bottom flange is divided into beam elements[14] with 6 degrees at each node.

c) As for the cross beam, the web is divided into quadrilateral plate elements with in-plane and out-of-plane displacements, and the top and bottom flanges are divided into beam elements with 6 degrees at each node.

d) The intermediate sway bracings are divided into beam elements with 6 degrees at each node.

To examine the effects of the sway bracings, stringers, steel plate attached to the bottom surface of the slab and the wall parapets, calculations are carried out for 6 structural models as shown in Table 1. Model I is a grid-girder model. In this model, it is assumed that the steel plate attached to the bottom surface of

Table 1 Structural models.

Structural model	Sway bracings	Stringers	Steel plate under slab	Wall parapets
I	N	N	C	N
II	N	N	N	N
III	C	N	N	N
IV	C	C	N	N
V	C	C	C	N
VI	C	C	C	C

Note C: Considered
N: Not considered

Table 2 Material constants.

Material	Young's modulus (MPa)	Poisson's ratio
Steel	0.206×10^6	0.3
Reinforced concrete	0.294×10^5	1/6

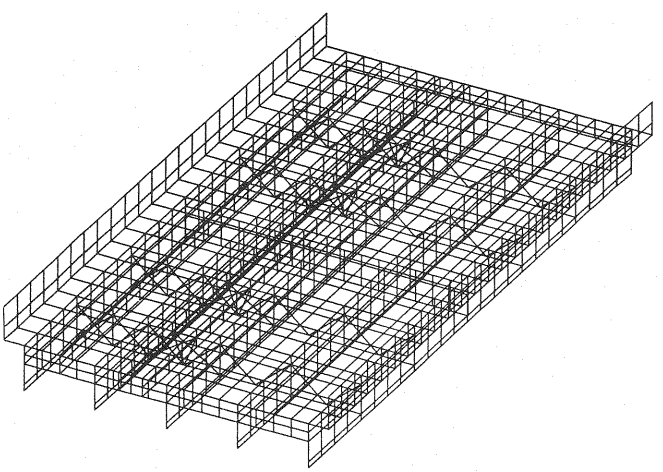

Fig. 13 Mesh division of Model VI.

the slab has a composite action for the main girders. The effective width of the slab complies with the provision in the Japanese Specification for Highway Bridges[12]. The structural models from II to VI are calculated by the aforementioned finite element method. In Models V and VI, the thickness of the steel plate attached to the bottom surface of the slab is converted into that of the concrete slab with the ratio of Young's moduli of both materials, and the former is added to the latter. In the plate girder bridge, a concrete wall 1 075 mm high and 250 mm thick is used for the parapets. Accordingly, in Model VI, they are divided into quadrilateral plate elements with in-plane and out-of-plane displacements. The mesh division of Model VI is shown in Fig. 13. Material constants of steel and reinforced concrete are listed in Table 2.

A comparison of calculated values with measured ones for the bottom flange stress at the middle of the girder G_1 is shown in Fig. 14. The maximum value of Model I is 1.75 times larger than the measured maximum value. The values plotted in the figure for Model II ~V are obtained only for the case where the center of the rear two wheel axles exists just above the cross beam. They are about 1.5 times larger than the measured maximum value, in spite of the difference among the models. Accordingly, the sway bracings, stringers and steel plate attached to the bottom surface of the slab do not contribute so much to load distribution. On the other hand, the maximum value of Model VI, in which the wall parapets are considered, is 1.07 times larger than the measured maximum value. It is much closer to the measured value. Accordingly, in the plate girder bridge, the wall parapets contribute greatly to the overall stiffness of the bridge.

The relation between the measured and analytical values may be expressed by the following linear form.

$$\sigma_{exp}=\alpha\sigma_{cal}+\beta \quad \cdots\cdots (11)$$

where σ_{exp} and σ_{cal} are the measured and analytical values, respectively, and α and β are coefficients. The values of α, β and correlation coefficient r determined by the least squares method are listed in Table 3 for Model I and VI. It can be seen that there are good correlations between the measured and analytical values.

(3) Effects of wall parapets on θ_{s0}

Let us examine the effects of the wall parapets on the rotation θ_{s0} which is due to the plate-bending deformation of the slab and which does not depend on vertical displacements of the main girders. As shown in Fig. 15, the wall parapets and slab of the plate girder bridge are divided into quadrilateral plate elements with in-plane and out-of-plane displacements. This finite element model is simply supported at the locations where the main girders exist. When a concentrated load is between the supporting lines of G_1 and G_2, the rotations at the points 1 and 2 on the supporting lines are smaller than those estimated by Eqs. (6) and (7). Multiplying Eqs. (6) and (7) by reduction factors ϕ_ρ, the rotations at

Table 3 Values of α, β in Eq. (11) and correlation coefficient r.

Main girder	Loading case	Structural model (I) α	β(MPa)	r	Structural model (VI) α	β(MPa)	r
G_1	A	0.623	-1.267	0.987			
	B	0.618	-0.989	0.991	0.958	-1.488	0.991
	C	0.615	-0.405	0.998	0.940	-0.012	0.992
	D	0.705	-0.808	0.998	1.040	-0.515	0.997
G_2	A	0.753	-1.342	0.964			
	B	0.781	-1.265	0.986	1.047	-1.838	0.989
	C	0.687	-0.427	0.965	0.891	-0.372	0.967
	D	0.700	-0.519	0.990	0.853	-0.684	0.990

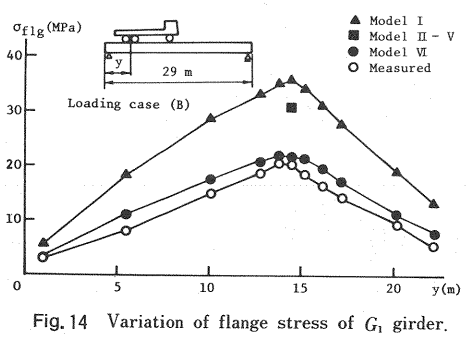

Fig. 14 Variation of flange stress of G_1 girder.

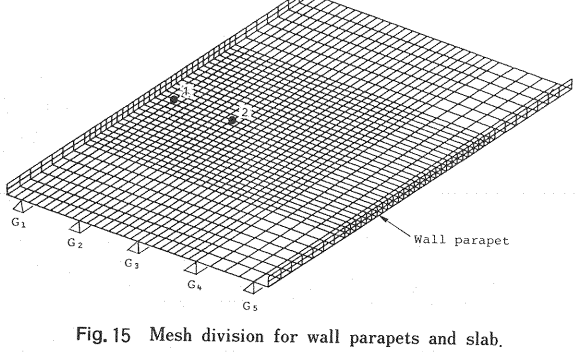

Fig. 15 Mesh division for wall parapets and slab.

the points 1 and 2 are given as follows.

$$\theta_{s01p}=\phi_{p12}\theta_{s01} \quad (12)$$

$$\theta_{s02p}=\phi_{p21}\theta_{s02} \quad (13)$$

where θ_{s01p} and θ_{s02p} are, respectively, the rotations at the points 1 and 2 due to the plate-bending deformation of the slab including the effects of the wall parapets, $\phi_{p12}=0.097\,x_{12}/a+0.518$, and $\phi_{p21}=0.334\,x_{12}/a+0.702$.

As can be seen from Eq. (12), the rotation due to the plate-bending deformation of the slab at the exterior main girder is reduced by half by the effects of the wall parapets.

(4) Relation between Δu_{sg} and θ_g

In the finite element model Ⅵ, let us examine the variation of γ defined by the following equation as the loading truck moves in the bridge-axis direction.

$$\gamma=\Delta u_{sg}/\theta_g \quad (14)$$

It can be seen from Fig. 16 that γ shows small variance for each loading position of B, C and D. Substituting γ into Eq. (3), the following equation is obtained for σ_{my} and σ_{by}.

$$\begin{bmatrix}\sigma_{my}\\ \sigma_{by}\end{bmatrix}=\begin{bmatrix}k_{m1} & k_{m1} & k_{m2}+k_{m3}\gamma\\ k_{b1} & k_{b1} & k_{b2}+k_{b3}\gamma\end{bmatrix}\begin{bmatrix}\theta_{s0}\\ \theta_{s1}\\ \theta_g\end{bmatrix} \quad (15)$$

(5) Relation between θ_{s1} and θ_g

θ_{s1} is the rotation of a slab produced by the vertical displacements of main girders. The rotation of the slab on the main girders given by the finite element analysis contains the rotation both due to the plate-bending deformation of the slab and due to the vertical displacement of the main girders. In the mesh division for the finite element analysis, the slab is divided into four elements between the main girders. Since the mesh division of such a degree is not enough to express the plate-bending deformation of the slab, the rotation given by the finite element analysis is not accurate to estimate θ_{s1}.

The vertical displacements of the cross beam and slab are equal at each cross beam connection. Regarding the slab as a continuous beam with a certain effective width just above the cross beam, the rotation of the slab produced by the vertical displacements of the main girders becomes equal to that of the cross beam given by Eq. (10). Accordingly, θ_{s1} will take a value close to θ_g. Then, as shown by the following equation, let us assume that θ_{s1} is equal to θ_g.

$$\theta_{s1}=\theta_g \quad (16)$$

Substituting Eq. (16) into Eq. (15), the following equation is obtained.

$$\begin{bmatrix}\sigma_{my}\\ \sigma_{by}\end{bmatrix}=\begin{bmatrix}k_{m1} & k_{m3}(\gamma-k_{m123})\\ k_{b1} & k_{b3}(\gamma-k_{b123})\end{bmatrix}\begin{bmatrix}\theta_{s0}\\ \theta_g\end{bmatrix} \quad (17)$$

where $k_{m123}=-(k_{m1}+k_{m2})/k_{m3}$ and $k_{b123}=-(k_{b1}+k_{b2})/k_{b3}$

(6) Relation between local stresses and three-dimensional behavior of bridge

By applying the least squares method to the following equation, the coefficients k_{m1}, k_{m3}, k_{m123}, k_{b1}, k_{b3} and k_{b123} in Eq. (17) are determined.

$$\begin{bmatrix}\sigma_{my}\\ \sigma_{by}\end{bmatrix}=\begin{bmatrix}k_{m1} & k_{m3}(\gamma-k_{m123})\\ k_{b1} & k_{b3}(\gamma-k_{b123})\end{bmatrix}\begin{bmatrix}\theta_{s0}\\ \theta_g\end{bmatrix}+\begin{bmatrix}c_m\\ c_b\end{bmatrix} \quad (18)$$

where c_m and c_b are constants.

33 measured values obtained at the loading positions of B, C and D are used for σ_{my} or σ_{by}. On the other hand, θ_{s0} and θ_g are calculated as follows.

a) For θ_{s0}

Calculating the rotation of the slab from Eqs. (12) and (13) for each wheel load of the loading truck, the sum of the rotations produced by 6 wheel loads is used for θ_{s0}. The plate thickness in the flexural rigidity D of the concrete slab in Eq. (12) and (13) is 180 mm, neglecting the composite action of the steel plate

attached to the bottom surface of the slab.

b) For θ_g

The rotation θ_g is calculated by the first or the second equation in Eq. (10), using the vertical displacements of the main girders at the cross beam connections which are obtained from the finite element analysis for Model VI.

As for γ, the values shown in Fig. 16 are used for each of the loading positions of B, C and D.

After an arbitrary value has been assumed for the coefficient k_{123} in Eq. (18), the least squares method is applied to Eq. (18). The variations of the multiple correlation coefficient r and the constant c against the coefficient k_{123} are shown in Fig. 17. The value of k_{123} when the multiple correlation coefficient r is close to one, and when the constant c is zero, and the values of k_1 and k_3 at those conditions are used for the values of the coefficients in Eq. (17). The obtained values of k_1, k_3, k_{123} and r are listed in Table 4. It can be seen from Table 4 that the multiple correlation coefficient r is very close to one. A comparison of

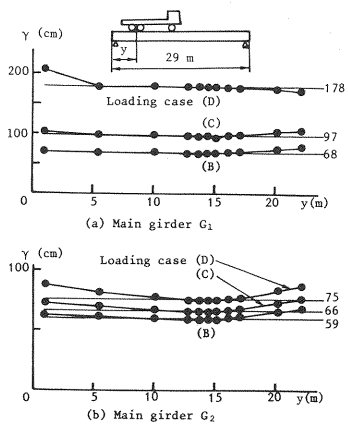

Fig. 16 Variation of γ.

Table. 4 Values of k_1, k_3, k_{123} in Eq. (17) and multiple correlation coefficient r.

Location of local stress	k_1 (MPa)	k_3 (MPa/cm)	k_{123} (cm)	r
1 (σ_{my})	-4.011×10^{4}	3.781×10^{2}	27	0.988
2 (σ_{my})	7.999×10^{4}	7.603×10^{2}	23	0.996
3 (σ_{by})	3.586×10^{4}	-1.232×10^{3}	79	0.990
4 (σ_{by})	1.831×10^{4}	-4.284×10^{2}	109	0.995

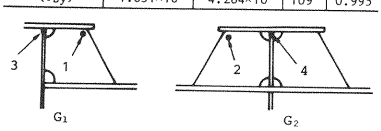

Table 5 Comparison of terms in Eq. (17).

Location of local stress	Loading case	$k_1\theta_{s0}$ (MPa) (1)	$k_3(\gamma_1-k_{123})\theta_g$ (MPa) (2)	Total value (MPa) (3)	Measured value (MPa) (4)	(1)/(3) (%) (5)
1 (σ_{my})	B	-19.8	-7.1	-26.9	-29.2	74
	C	-28.9	-8.1	-37.0	-38.3	78
	D	-29.3	-9.0	-38.3	-35.9	77
2 (σ_{my})	B	-35.6	-14.2	-49.8	-48.9	71
	C	-49.0	-14.4	-63.4	-65.7	77
	D	-56.3	-14.7	-71.0	-72.2	79
3 (σ_{by})	B	17.7	-5.9	11.8	10.2	150
	C	25.9	6.8	32.7	32.3	79
	D	26.2	19.2	45.4	43.5	58
4 (σ_{by})	B	-8.1	-10.8	-18.9	-19.3	43
	C	-11.2	-8.1	-19.3	-18.7	58
	D	-12.9	-5.2	-18.1	-18.0	71

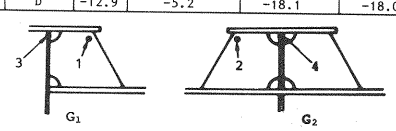

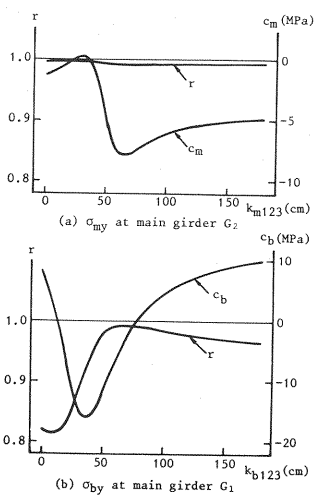

Fig. 17 Variation of r and c against k_{123}.

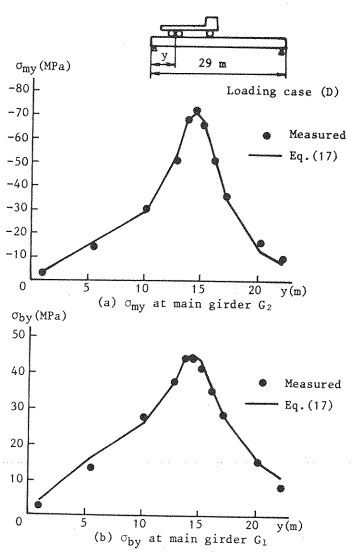

Fig. 18 Comparisons between the values of Eq. (17) and the measured ones.

the values estimated by Eq. (17) with the measured ones is shown in Fig. 18 for the membrane stress σ_{my} at the connection plate of G_2 girder and the plate-bending stress σ_{by} at the web of G_1 girder. It can be seen that Eq. (17) is very close to the measured values.

A comparison of the terms in Eq. (17) is shown in Table 5. The values in the table are shown for the case where the center of the rear wheel axles exists just above the cross beam. The ratio of the $k_1\theta_{s0}$ value against the total value of the membrane stress σ_{my} at the connection plate is about 80%, and for the plate-bending stress σ_{by} at the main girder web the ratio is about 60%. Therefore, the rotations of the slab due to its plate-bending deformation and of the cross beam caused by the different vertical deflections of the main girders are equally influential for σ_{by}, while only the former has a great influence on σ_{my}.

4. CONCLUSION

In this paper, the relation between the local stresses which induced fatigue cracks at cross beam connections and the three-dimensional behavior of plate girder bridges was formulated by the results of the stress measurement of an actual plate girder bridge and its three-dimensional finite element analysis. The obtained equation revealed the influential factors for the occurrence of the local stresses.

ACKNOWLEDGEMENTS

We would like to thank Prof. Y. Maeda, Kinki University, for his valuable comments on this paper. We would also like to thank Mr. H. Saito, Hanshin Expressway Public Corporation, for his remarks in the finite element analysis, and Mr. H. Hayashi, the same Corporation, for his help with the data acquisition.

REFERENCES

1) Nishikawa, K. : Fatigue problems in highway bridges, pp. 19~23. Abe, H. et al. : Fatigue problems in railway bridges, pp. 24~29. Miki, T. and Fisher, J. W. : Fatigue problems in foreign bridges, pp. 30~34. The Bridge and Foundation Engineering, Kensetsutosho Publisher, Tokyo, Vol. 17, No. 8, 1983. (in Japanese)
2) Fisher, J. W. : Fatigue and Fracture in Steel Bridges, John Wiley & Sons, Inc., 1984.
3) Akashi, S. : Fatigue crackings and their researches of welded structures, Proc. of JSCE, No. 350, pp. 1~7, 1984. (in Japanese)
4) Hanshin Expressway Public Corp. and Naigaikoei Co., Ltd. : Classification of Fatigue Cracks at Member Connections in Plate Girder Bridges, Mar., 1985. (in Japanese)
5) Saeki, S., Nishikawa, K. and Takizawa, A. : Report on Loading Tests of Kyowa Bridge, Technical Note of Public Works Research Institute, Ministry of Construction, Japan, No. 2123, Jun., 1984. (in Japanese)
6) Hanshin Expressway Public Corp. and Kawasaki Heavy Industries, Ltd. : Investigation on Fatigue of Main Girder and Cross Beam Connections in Composite I-Girder Briges···Part 2, Mar., 1985. (in Japanese)
7) Sinohara, Y., Nishikawa, K. and Takizawa, A. : Measurement of Stress History of Composite H-Beam Bridge Suffering from Fatigue Damage, Technical Note of Public Works Research Institute, Ministry of Construction, Japan, No. 2344, Mar., 1986. (in Japanese)
8) Fisher, T. A., Fisher, J. W., Kostem, C. N. and Mertz, D. R. : Design and retrofit for fatigue damage in web gap, IABSE Colloquium, Lausanne, pp. 535~543, 1982.
9) Kato, S., Yoshikawa, O., Terada, H. and Matsumoto, Y. : Studies on fatigue damages based on strain measurements of a highway bridge, Proc. of JSCE Struct. Eng. /Earthq. Eng., Vol. 2, No. 2, Japan Society of Civil Engineers, pp. 445s~454s, 1985.
10) Okura, I., Hirano, H. and Yubisui, M. : Stress measurement at cross beam connections of plate girder bridge, Technol. Repts. Osaka Univ., Vol. 37, No. 1883, pp. 151~160, 1987.
11) Timoshenko, S. P. and Woinowsky-Krieger, S. : Theory of Plates and Shells, Second Edition, McGraw-Hill, p. 145, 1959.
12) Japan Road Association : Specification for Highway Bridges, 1964. (in Japanese)
13) Zienkiewicz, O. C. and Cheung, Y. K. : The Finite Element Method in Structural and Continuum Mechanics, McGraw-Hill, pp. 66~67, pp. 90~98 and pp. 124~137, 1967.
14) Sanbongi, S. and Yoshimura, N. : Structure Analysis Program by Finite Element Method, Baihukan Publisher, Tokyo, p. 51, 1970. (in Japanese)

(Received May 19 1987)